Journal of Statistical Physics, Vol. 10, No. 5, 1974

Irreversible Behavior of Interacting Systems. II. Fluctuations in Equilibrium

George Mandeville[1] and Michael Coopersmith[1]

Received October 11, 1973

The mathematical techniques of the previous paper are used to calculate the fluctuations of the order parameter for large, finite Kac ring models and their subsystems. It is shown that the fluctuations have a characteristic frequency even in the thermodynamic limit. This indicates that a prepared state far from equilibrium does not behave like a large fluctuation. A simplified version of the Fourier spectrum of the fluctuations is also presented which contains all the general features of finite Kac models and is more amenable to analysis.

KEY WORDS: Nonequilibrium system; fluctuations; Fourier transform; time–space symmetry; Kac ring model; characteristic frequency.

1. INTRODUCTION

There is usually sufficient difficulty in determining the behavior of the ensemble averages in a nonequilibrium model that one does not attempt any direct calculation of the fluctuations from these averages. Fluctuations are not completely ignored, but are considered most often in a qualitative manner involving an order-of-magnitude calculation and some intuitive reasoning.[1] Usually, the order of magnitude of the fluctuations will be the inverse square

[1] Physics Department, University of Virginia, Charlottesville, Virginia.

root of the number of particles. In the thermodynamic limit the fluctuations are therefore small and, for most considerations, negligible.

The qualitative behavior of fluctuations is important when one is considering long periods of time. During sufficiently long observation periods the probability that a sizable fluctuation will occur is no longer negligible. The question then arises, "Will the system return to equilibrium from a large fluctuation in the same way that it returns to equilibrium from a prepared state?" The usual answer to this is "yes" with the additional statement, to eliminate the paradox of irreversibility, that any large deviation from equilibrium is with overwhelming probability an extremum, allowing one to ignore any inference of a preferred time direction.

The Kac model as an example of a very simple irreversible model contradicts this answer in some respects. The detailed analysis that follows indicates that the fluctuations are not random excursions from equilibrium, but demonstrate *definite periodic behavior. This raises doubt that the return from a large deviation will appear identical to the return from a prepared state.*

There is a great deal of time–position symmetry in the Kac model. Figure 1 shows the complete history for one model, illustrating this sym-

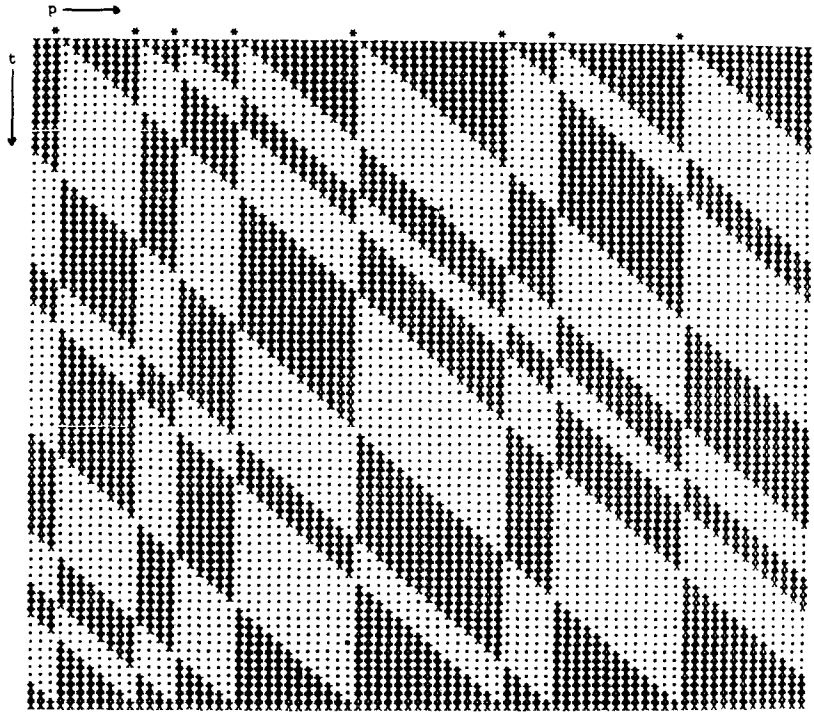

Fig. 1. Position–time symmetry in the Kac model.

metry. In fact, if we perform the map

$$\eta_p(t) \to f(p, t + p) \tag{1}$$

we obtain a function $f(x, y)$ which is completely symmetric in x and y when $\eta_p(0) = 1$. That is,

$$f(x, y) = f(y, x) \qquad \text{if} \quad f(x, x) = 1 \tag{2}$$

This symmetry between time and position leads one to expect correlations between characteristic lengths and characteristic periods. In the next section we find this to be the case.

2. CHARACTERISTIC FLUCTUATIONS OF KAC MODELS

The ensemble average of the order parameter is representative of particular Kac models in that it reflects the characteristic relaxation time and Poincaré cycle. It is not representative, however, of the fluctuations of typical Kac models. The ensemble averaging cancels the fluctuations observed in particular systems and is of no value in studying the characteristic frequency distribution of Kac models. Exact solutions of particular models (Fig. 2) show that the frequency distribution is not uniform and appears to be related to scatterer density. The following is an analysis of that dependence.

To simplify the discussion, we restrict the analysis to large Kac models with an even number of scatterers. A similar analysis can be done for odd numbers, but it does not further illuminate the subject. The deviation of the order parameter from its expected value can be expressed as

$$\Gamma(t) - \langle \Gamma(t) \rangle = \sum_{k=1}^{n} a_k \cos(2\pi kt/n) \tag{3}$$

where the Fourier transform a_k is given by

$$a_k = (1/n) \sum_{t=1}^{n} [\Gamma(t) - \langle \Gamma(t) \rangle] \cos(2\pi kt/n) \tag{4}$$

Ideally, we would like to obtain $\langle |a_k| \rangle$, the characteristic magnitude of the Fourier components. Unfortunately, this quantity does not yield readily to calculation. A related quantity, $\langle a_k^2 \rangle^{1/2}$, can be calculated, however, and represents a good estimate of the form, if not the magnitude, of $\langle |a_k| \rangle$. We write

$$\begin{aligned} \langle a_k^2 \rangle &= \frac{1}{n^2} \sum_{tt'} \langle \Gamma(t)\Gamma(t') - \langle \Gamma(t) \rangle \langle \Gamma(t') \rangle \rangle \cos \frac{2\pi kt}{n} \cos \frac{2\pi kt'}{n} \\ &= \frac{1}{n^2} \sum_{tt'} \langle \Gamma(t)\Gamma(t') \rangle \cos \frac{2\pi k(t - t')}{n} \\ &\quad - \frac{1}{n^2} \left[\sum_{t} \langle \Gamma(t) \rangle \cos \frac{2\pi kt}{n} \right]^2 \end{aligned} \tag{5}$$

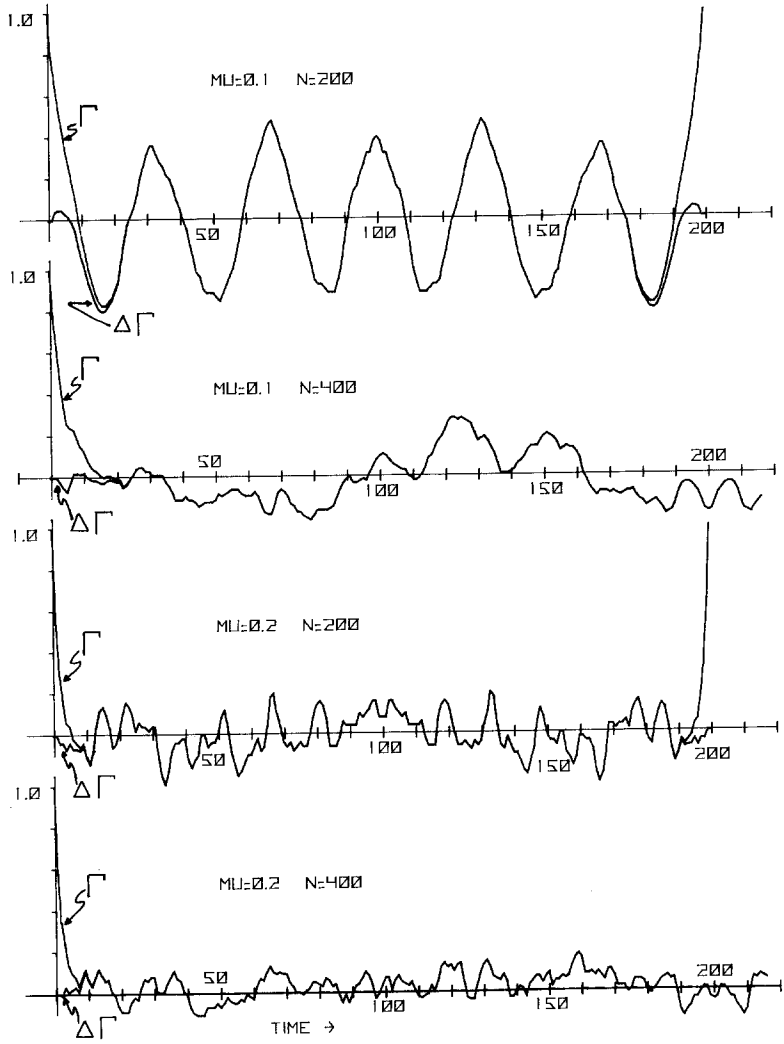

Fig. 2. Typical order parameter behavior for finite systems.

where use has been made of the evenness of $\Gamma(t)$, i.e.,

$$\sum_t \Gamma(t) \sin(2\pi kt/n) = 0 \tag{6}$$

The crucial point in the calculation is the substitution of expressions for the ensemble averages in the right-hand side of (5). A fruitful approach is to

note that for $n \gg 1$ and $\mu < \frac{1}{2}$ we can use the approximate form in the preceding paper,

$$\sum_s (-1)^s G(s) \approx (1 - 2\mu)^t + (1 - 2\mu)^{n-t} \tag{7}$$

and write (5) as

$$\begin{aligned}\langle a_k^2 \rangle = (1/n^4) \sum_{tt'pp'} (z^\Delta + z^{n-\Delta}) \cos[\kappa(t - t')] \\ - [(1/n^2) \sum_{tp} (z^t + z^{n-t}) \cos(\kappa t)]^2\end{aligned} \tag{8}$$

where $\kappa \equiv 2\pi k/n$, $z \equiv 1 - 2\mu$, and Δ is the number of ϵ's occurring once in the chain $\epsilon_{p+1} \cdots \epsilon_{p+t}\epsilon_{p'+1} \cdots \epsilon_{p'+t'}$.

With the aid of diagrams (Appendix A) these sums can be expressed as

$$\begin{aligned}\langle a_k^2 \rangle = (1/n^3)\Bigg\{ &\sum_{t=1}^{n-1} \sum_{q=t}^{n-1} \sum_{t'=1}^{n-q} (z^{t+t'} + z^{n-t-t'}) \cos[\kappa(t - t'])] \\ &+ 2 \sum_{t=2}^{n=1} \sum_{q=1}^{t-1} \sum_{t'=t-q+1}^{n-q} (z^{2q+t'-t} + z^{n-2q-t'+t}) \cos[\kappa(t - t')] \\ &+ 2 \sum_{t=1}^{n} \sum_{q=0}^{t-1} \sum_{t'=1}^{t-q} (z^{t-t'} + z^{n-t+t'}) \cos[\kappa(t - t')] - n \\ &+ \sum_{t=2}^{n} \sum_{q=1}^{t-1} \sum_{t'=n-q+1}^{n} (z^{2n-t-t'} + z^{t+t'-2n}) \cos[\kappa(t - t')] \Bigg\} \\ &- \left[(1/n) \sum_{t=1}^{n} (z^t + z^{n-t}) \cos(\kappa t) \right]^2\end{aligned} \tag{9}$$

which after a laborious calculation gives

$$\langle a_k^2 \rangle = \frac{1}{n^2} \left[\frac{1 - z^2}{1 + z^2 - 2z \cos \kappa} \right]^2 + O\left(\frac{1}{n^3}\right) \tag{10}$$

Figure 3 is a plot of $\langle a_k^2 \rangle^{1/2}$ for various densities. The general form is that of a low-pass filter with very small contributions for all but low frequencies. The cutoff frequency can be approximated by calculating the point at which $\langle a_k^2 \rangle^{1/2}$ drops to one-half its initial value. We obtain

$$1/(1 - z)^2 = 2/(1 + z^2 - 2z \cos \kappa) \tag{11}$$

For dilute systems this is

$$\kappa \approx 2m/n \tag{12}$$

The cutoff period associated with this value of κ is

$$\tau \equiv n/k = 2\pi/\kappa \approx \pi n/m \tag{13}$$

which compares favorably with the oscillatory behavior for particular Kac models, as seen in Fig. 2.

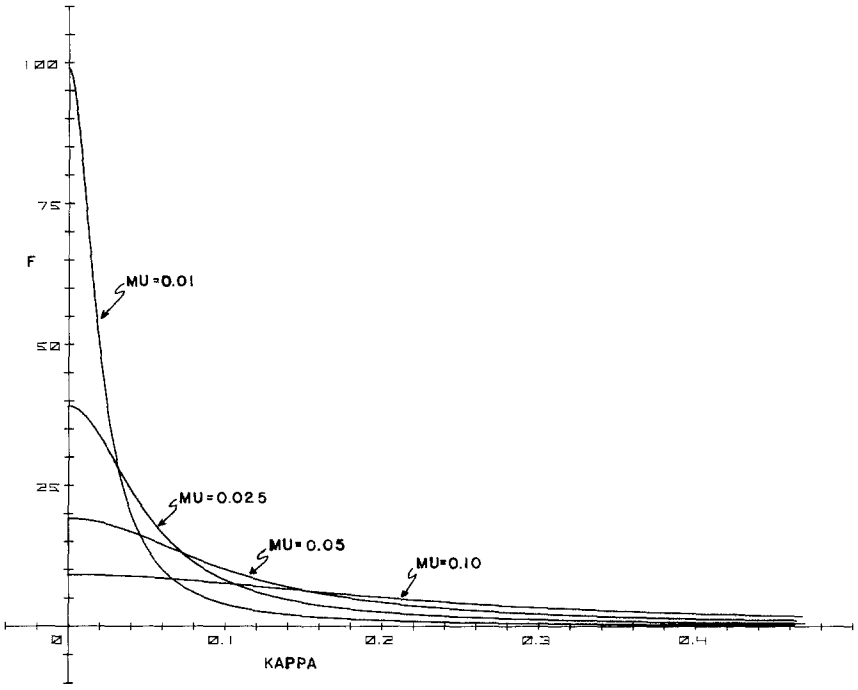

Fig. 3. Frequency distributions for Kac models of various densities. $F = n\langle a_k^2\rangle^{1/2}$.

We have seen that the fluctuations of a Kac model are not representative of a random process, but exhibit periodic behavior. It is especially significant that this periodic behavior is strictly a function of the density of scatterers and is not a function of the size of the system. Therefore, *density-dependent periodicity exists even in the thermodynamic limit* and is a characteristic feature of a typical ensemble member as well as the ensemble average.

3. CHARACTERISTIC FLUCTUATIONS OF SUBSYSTEMS

To complete the comparison of subsystem and whole system behavior, we repeat the calculation of Section 2 for $\Gamma_s(t)$. The calculation is somewhat more complicated because the chains of ϵ's occurring in the calculation fall both inside and outside of the subsystem. We write, as before,

$$\langle a_k^2\rangle = (1/n^2)\sum_{t=1}^{n}\sum_{t'=1}^{n}\langle\Gamma_s(t)\Gamma_s(t')\rangle\cos[\kappa(t-t')] - \left[(1/n)\sum_{t=1}^{n}\langle\Gamma_s(t)\rangle\cos(\kappa t)\right]^2 \tag{14}$$

where the limits reflect the Poincaré cycle n (m is assumed even). By analogy with (7), we can write

$$\langle \epsilon_{p+1} \cdots \epsilon_{p+t} \epsilon_{p'+1} \cdots \epsilon_{p'+t'} \rangle \approx (z_s^{\Delta} + z_s^{n_s - \Delta_s})(z^{\Delta} + z^{n - n_s - \Delta}) \tag{15}$$

where

$$\Delta = \text{number of unpaired } \epsilon\text{'s outside the subsystem} \tag{16a}$$

$$\Delta_s = \text{number of unpaired } \epsilon\text{'s inside the subsystem} \tag{16b}$$

Using a diagram method (Appendix B) to reduce the summations to a manageable form, we obtain

$$\begin{aligned}
\langle a_k^2 \rangle = \frac{1}{(n_s n)^2} \Bigg\{ & 2 \sum_{p=1}^{n_s-2} \sum_{t=1}^{n_s-p-1} \sum_{p'=p+t}^{n_s-1} \sum_{t'=1}^{n_s-p'} z_s^{t+t'} \cos[\kappa(t-t')] \\
& + 2 \sum_{p=1}^{n_s-2} \sum_{t=2}^{n_s-p+1} \sum_{p'=p+1}^{p+t-1} \sum_{t'=p+t-p'+1}^{n_s-p'} z_s^{2p'-2p+t'-t} \cos[\kappa(t-t')] \\
& + 2 \sum_{p=1}^{n_s-1} \sum_{t=n_s-p+1}^{n-p-1} \sum_{p'=p+1}^{n_s} \sum_{t'=p+t-p'+1}^{n-p} z^{p'+t'-p-t} z_s^{p'-p} \cos[\kappa(t-t')] \\
& + 2 \sum_{p=1}^{n_s-1} \sum_{t=n-p+1}^{n-1} \sum_{p'=p+1}^{n_s} \sum_{t'=p+t-p'+1}^{n-p'+p} z_s^{2p'-2p+t'-t} \cos[\kappa(t-t')] \\
& + 2 \sum_{p=1}^{n_s-1} \sum_{t=1}^{n_s-p'} \sum_{p'=p}^{p+t-1} \sum_{t'=1}^{p-p'+t} z_s^{t-t'} \cos[\kappa(t-t')] \\
& + 2 \sum_{p=1}^{n_s-1} \sum_{t=n-p+1}^{n} \sum_{p'=p}^{n_s-1} \sum_{t'=1}^{n_s-p} z_s^{n-t+t'} \cos[\kappa(t-t')] \\
& + 2 \sum_{p=1}^{n_s} \sum_{t=n_s-p+1}^{n-p} \sum_{p'=p}^{n_s} \sum_{t'=n_s-p'+1}^{t-p'+p} z^{p+t-p'-t'} z_s^{p'-p} \cos[\kappa(t-t')] - n^2 \\
& + 2 \sum_{p=1}^{n_s-1} \sum_{t=n-p+1}^{n} \sum_{p'=p}^{n_s} \sum_{t'=n-p'+p+1}^{p+t-p'} z_s^{t-t'} \cos[\kappa(t-t')] \\
& + 2 \sum_{p=1}^{n_s-1} \sum_{t=n-p+1}^{n} \sum_{p'=p+1}^{n_s} \sum_{t'=n-p'+p+1}^{n} z_s^{2n-t'-t} \cos[\kappa(t-t')] - n_s n \Bigg\} \\
& - \left\{ \frac{1}{n n_s} \sum_{p=1}^{n_s} \left[\sum_{t=1}^{n_s-p} z_s^{t} \cos(\kappa t) + \sum_{t=n-p+1}^{n} z_s^{n-t} \cos(\kappa t) \right] \right\}^2
\end{aligned} \tag{17}$$

After considerable calculation, this expression reduces to

$$\begin{aligned}
\langle a_k^2 \rangle = & \frac{1}{n^2 n_s} \left[(n - n_s) \frac{1 - z^2}{1 + z^2 - 2z \cos \kappa} + n_s \frac{1 - z_s^2}{1 + z_s^2 - 2 z_s \cos \kappa} \right] \\
& \times \frac{1 - z_s^2}{1 + z_s^2 - 2z \cos \kappa}
\end{aligned} \tag{18}$$

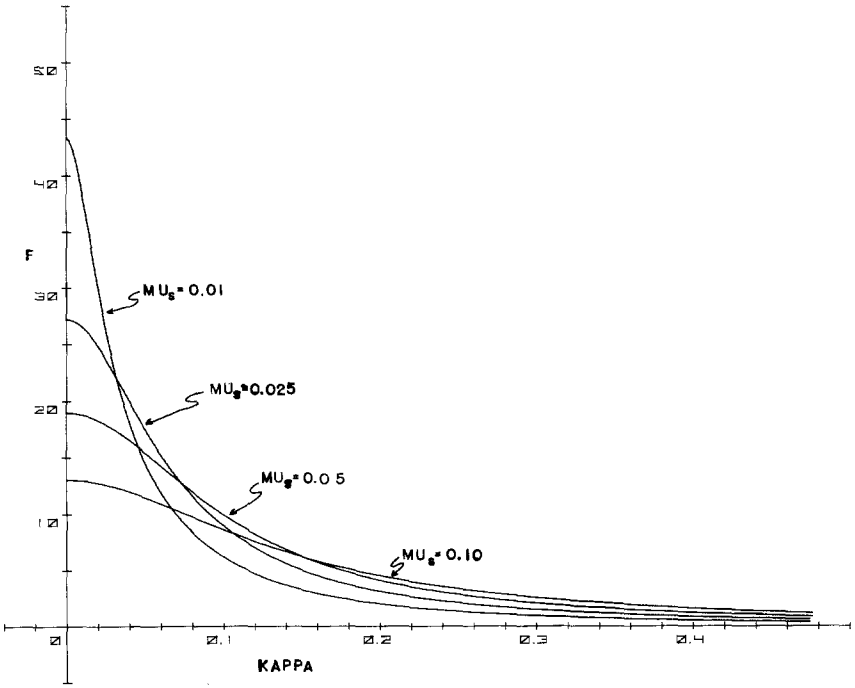

Fig. 4. Frequency distributions for Kac model subsystems of various densities. $F = n^{1/2}n_s^{1/2}\langle a_k^2\rangle^{1/2}$; $\mu = 0.05$.

The case of greatest interest is the one in which μ and μ_s are significantly different. In this case $n_s \ll n$ because a subsystem which is a finite fraction of the whole system will not have a significant density difference. Figure 4 shows the form of this function for different densities.

We have seen that the fluctuations of a subsystem are dependent equally on the scatterer density internal to the subsystem and the external scatterer density, when the subsystem is small compared with the whole system. Once again the form of the frequency distribution does not depend upon the size of the whole system, and the periodicity persists in the thermodynamic limit.

4. A MODEL OF THE KAC MODEL

The foregoing analysis leads us to the following simplified picture (or, alternatively, a new one-dimensional model). The Fourier spectrum has been shown to have a magnitude which looks qualitatively like Fig. 3. This can be approximated by a rectangular distribution of $|a_k|$ with a width equal to k_0. From Eq. (13) this is approximately m/π. The phases of the cosines are

randomly 0 or π, that is, the coefficients of the cosines are randomly plus or minus one with the constraint that the sum of the coefficients is zero. Formally, we have

$$\Gamma(t) - \langle\Gamma(t)\rangle = \sum_{k=1}^{k_0} \cos(kt + \psi_k) \tag{19}$$

where $\psi_k = 0$ or π and $\sum_{k=0}^{k_0} \psi_k = \frac{1}{2}\pi k_0$.

The expression given by Eq. (19) illustrates the low-pass filter aspect of the Fourier spectrum but, more importantly, allows for algebraic (rather than numerical) analysis. Thus we can demonstrate that the qualitative appearance of $\Gamma(t) - \langle\Gamma(t)\rangle$, as shown in Fig. 2, from numerical calculations of a specific arrangement of scatterers is indicative of most members of the ensemble. To do this, we make use of an expression developed by Kac[2] for the frequency of zeros of a general function and adapted by Slater[3] to find the behavior of a sum of vibrations of the form of Eq. (19).[2]

The expression with which Kac starts for the number of zeros in the interval $(0, T)$ is

$$\begin{aligned} G(T; \psi_1, \ldots) &= \pi^{-1} \int_0^\infty dx \int_0^T \cos[xf(t)]|f'(t)|\, dt \\ &= 2\pi^{-2} \int_0^\infty dx \int_0^T y^{-2}\, dy \int_0^T \cos[xf(t)]\{1 - \cos[yf'(t)]\}\, dt \end{aligned} \tag{20}$$

where $f(t)$ is a function with continuous derivative and finite number of zeros in the interval $(0, T)$ and we have used Slater's formula for $|f'(t)|$.[3] For the phase-average frequency of zeros, L, in $(0, T)$ we have

$$\begin{aligned} L &= \frac{1}{2^{k_0}T} \sum_{\psi_1=0}^{\pi} \cdots \sum_{\psi_{k_0}=0}^{\pi} G(T; \psi_1, \ldots) \\ &= \frac{1}{\pi^2 2^{k_0-1}T} \int_0^\infty dx \int_0^\infty y^{-2}\, dy \int_0^T \sum_{\psi_1=0}^{\pi} \cdots \sum_{\psi_k=0}^{\pi} \cos\left[x \sum_{k=1}^{k_0} \cos(\kappa t + \psi_k)\right] \\ &\quad \times \left\{1 - \cos\left[\kappa y \sum_{k=1}^{k_0} \sin(\kappa t + \psi_k)\right]\right\} dt \\ &= \frac{2}{\pi^2 T} \int_0^\infty dx \int_0^\infty y^{-2}\, dy \int_0^T \left(\prod_{k=1}^{k_0} \cos[x \cos(\kappa t)]\right. \\ &\quad \times \left\{1 - \prod_{k=1}^{k_0} \cos[\kappa y \sin(\kappa t)]\right\} \\ &\quad \left. + \text{terms involving } \sin[x \cos(\kappa t)] \sin[\kappa y \sin(\kappa t)]\right) dt \end{aligned} \tag{21}$$

[2] We are indebted to Prof. S. A. Rice for calling this obscure work to our attention.

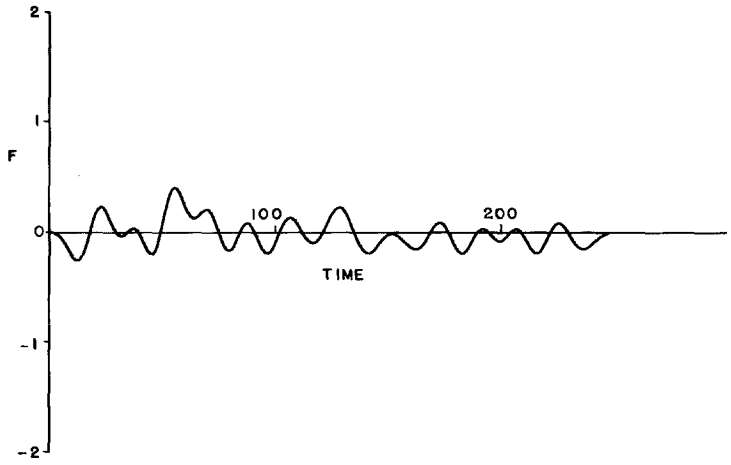

Fig. 5. Random sum of 26 cosines.

where we have put $f(t) = \Gamma(t) - \langle\Gamma(t)\rangle$. The last expression is obtained by expanding the cosines of sums and performing the phase averages. The phase-average frequency of zeros is nearly equal to the frequency of zeros of the function $g(t) = \sum_{k=1}^{k_0} \cos(\kappa t)$, that is, the sum of cosines with all positive coefficients, when the time T is taken to be the Poincaré cycle time n. We do not have a rigorous proof of this last statement but we give a heuristic argument for it in Appendix C. In any case, the number of zeros of $g(t)$ in $(0, n)$ agrees very well with the number of zeros of $\Gamma(t) - \langle\Gamma(t)\rangle$ in Fig. 2.

To calculate this number, note that $g(t)$ can be written as

$$g(t) = \frac{1}{2}\frac{\sin[(2k_0 + 1)\pi t/n] - \sin(\pi t/n)}{\sin(\pi t/n)} \tag{22}$$

The number of zeros of $g(t)$ in the interval $(0, n)$ is clearly $2k_0$. For the case of 20 scatterers ($m = 20$) $2k_0 = 40/\pi \approx 13$, which (probably fortuitously!) is identical to the number of zeros of the first graph ($\mu = 0.1$, $n = 200$) in Fig. 2. A more detailed comparison with the Kac model shown in the last graph of Fig. 2 ($\mu = 0.2$, $n = 400$) is made in Fig. 5. Here we have plotted $f(t)$ for a random arrangement of plus and minus signs with $k_0 = 26$. Note that there are only 33 zeros in $(0, n)$ as opposed to the estimated value of 52 from the corresponding $g(t)$.

5. CONCLUDING REMARKS

While the results of the previous paper seem to be in accord with physical systems, it seems likely that the results in this paper concerning periodicity

may not be a general feature of such systems. This is probably due to the nonergodicity of the Kac model. More precisely, the system development of the Kac model does not cover all of the available phase space. Thus, a large fluctuation is not equivalent to a prepared state far from equilibrium if the prepared state cannot be reached from the initial configuration. Whether this is a specific property of one-dimensional models such as the Kac model is a problem whose answer clearly requires further investigation.

APPENDIX A. FLUCTUATION DIAGRAMS FOR THE KAC MODEL

The calculation of (8) is made simpler by considering the summand in the first term as the product of two chains of ϵ's placed on a ring. We desire to perform the sum over all positions and lengths of the chains. The rotational symmetry of the ring allows us to carry out the p sum for all diagrams without complication. Introducing $q \equiv p' - p$, we are left with a triple sum in the

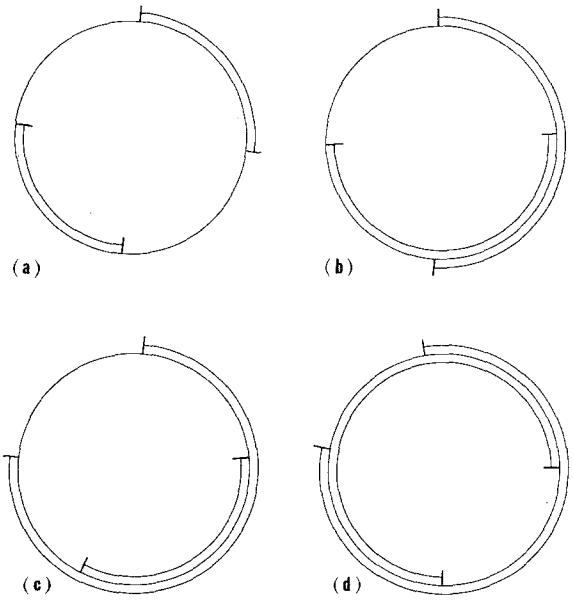

Fig. 6. (a) Diagram A. Nonoverlapping chains. $1 \leqslant t \leqslant n-1$; $t \leqslant q \leqslant n-1$; $1 \leqslant t' \leqslant n-q$. (b) Diagram B. Singly overlapping chains. $2 \leqslant t \leqslant n-1$; $1 \leqslant q \leqslant t-1$; $t-q+1 \leqslant t' \leqslant n-q$. (c) Diagram C. One chain enveloping another chain. $1 \leqslant t \leqslant n$; $0 \leqslant q \leqslant t-1$; $1 \leqslant t' \leqslant t-q$. (d) Diagram D. Doubly overlapping chains. $2 \leqslant t \leqslant n$; $1 \leqslant q \leqslant t-1$; $n-q+1 \leqslant t' \leqslant n$.

variables t, q, and t'. Figure 6 shows four diagrams which represent the possible configurations of these chains and express the associated conditions on the summation variables.

Each diagram consists of a fixed ring with an outer chain representing the positions $\epsilon_1, \epsilon_2, \ldots, \epsilon_t$ and an inner chain representing the positions $\epsilon_{q+1}, \epsilon_{q+2}, \ldots, \epsilon_{q+t'}$. The summations are carried out for each diagram allowing t, q, and t' to run over all values consistent with the diagram configuration.

The diagrams allow us to express Δ in terms of the summation indices. Counting the number of singly occurring ϵ's yields

$$\Delta = t + t' \qquad \text{for diagram A}$$

$$\Delta = 2q + t' - t \qquad \text{for diagram B}$$

$$\Delta = t - t' \qquad \text{for diagram C}$$

$$\Delta = 2n - t - t' \qquad \text{for diagram D}$$

Diagrams B and C do not include all the cases of single overlap and envelopment. This can be seen by reversing the inner and outer chains. We can correct for this error by counting each of these diagrams twice (for the two possible orientations) and subtracting the overcount which occurs for $q = 0$, $t = t'$ in diagram C. The overcount can be expressed as

$$\sum_{t=1}^{n} (z^{t-t'} + z^{n-t+t'}) \cos[\kappa(t - t')] = n, \qquad t = t' \tag{A.1}$$

where use has been made of the asymptotic form

$$z^n \ll 1 \qquad \text{for large } n \tag{A.2}$$

Equation (9) follows immediately from the diagrams. The calculation is best carried out by substituting

$$\cos[\kappa(t - t')] = \mathrm{Re}[e^{i\kappa(t-t')}] \tag{A.3}$$

and performing sums on quantities of the form x^t, where x is a complex number.

The exponential form of the summand implies that the significant contribution will occur at $\Delta \sim 0$ and $\Delta \sim n$, which correspond to almost no singly occurring ϵ's and almost all singly occurring ϵ's, respectively. In addition, these extremes must be associated with a free sum of at least one variable to contribute to the sum. By this reasoning one can discard the second

terms in A and B by inspection. This consideration plays a larger role in Appendix B.

APPENDIX B. FLUCTUATION DIAGRAMS FOR A KAC MODEL SUBSYSTEM

A method similar to that described in Appendix A can be applied to the Kac model subsystems. An additional complication arises from the asymmetry of two distinct regions on the ring diagrams. Each chain of ϵ's must terminate in the region associated with the subsystem, but the other ends of the chains can be in either of the regions. The diagram method of Appendix A is modified by introducing two radial lines to denote the subsystem region. The diagrams (Fig. 7) represent all configurations of chains terminating in the subsystem region. An additional subdivision of the Appendix A configurations is necessary to account for all the distinct configurations in the case of subsystems.

The only diagrams that contribute to the highest order of the calculation are those in which the empty ($\Delta \sim 0$) and the full ($\Delta \sim n$) limits have two degrees of freedom. This is necessary for the diagrams to generate a term of order n^2. The diagrams for which $\Delta_s \sim 0$ include A_1, B_1, B_4, B_6, C_1, C_4, C_6, and D_3. The diagrams for which $\Delta_s \sim n_s$ include B_4 and C_4. There are no contributing diagrams for which $\Delta \sim n - n_s$.

All the diagrams are doubly degenerate because distinct diagrams are obtained when the inner and outer chains are interchanged. Again an overcount results in C_1, C_4, and C_6 diagrams, but this is easily subtracted out of the sum.

The A_3, B_3, and D_1 diagrams do not contribute to order n^2 and are consequently left out of (17). The remaining diagrams are expressed in their summation form in (17) in the order given here. Diagrams A_1, B_1, C_1, C_3, C_6, and D_3 give the term that corresponds to the whole system, and diagrams B_4 and C_4 yield the new term.

APPENDIX C. FREQUENCY OF ZEROS OF $f(t)$

We wish to demonstrate that the phase-average frequency of zeros $f(t) = \sum_{k=1}^{k_0} \cos(\kappa t + \psi_k)$ is given to a good approximation by the frequency of zeros of $g(t) = \sum_{k=1}^{k_0} \cos(\kappa t)$, $\kappa = 2\pi k/n$. The argument is based on the apparent smallness of certain integrals, although we have no general estimate for their size. In view of the fact that we have no general proof, we will compare the expressions for the frequency of zeros of $f(t)$ and $g(t)$ for $k_0 = 4$. Even in this simple case, we can only make a heuristic argument for the size of the terms involved.

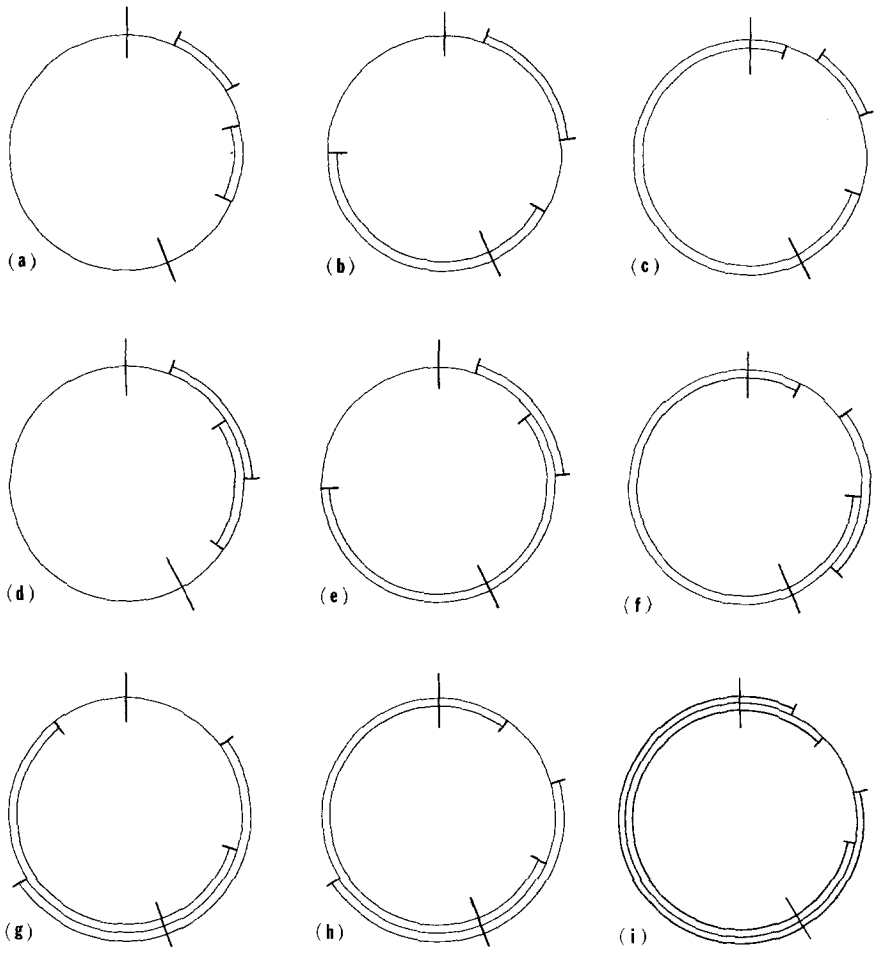

Fig. 7. (a) Diagram A_1. $1 \leqslant p \leqslant n_s - 2$; $1 \leqslant t \leqslant n_s - p - 1$; $p + t \leqslant p' \leqslant n_s - 1$; $1 \leqslant t' \leqslant n_s - p'$; $\Delta_s = t + t'$; $\Delta = 0$. (b) Diagram A_2. $1 \leqslant p \leqslant n_s - 1$; $1 \leqslant t \leqslant n_s - p$; $p + t \leqslant p' \leqslant n_s$; $n_s - p' + 1 \leqslant t' \leqslant n - p'$; $\Delta_s = t + n_s - p'$; $\Delta = p + t - n_s$. (c) Diagram A_3. $1 \leqslant p \leqslant n_s - 1$; $1 \leqslant t \leqslant n_s - p$; $p + t \leqslant p' \leqslant n_s$; $n - p' + 1 \leqslant t' \leqslant n - p' + p$; $\Delta_s = t + t' - n + n_s$; $\Delta = n - n_s$. (d) Diagram B_1. $1 \leqslant p \leqslant n_s - 3$; $2 \leqslant t \leqslant n_s - p + 1$; $p + t \leqslant p' \leqslant p + t - 1$; $p + t - p' + 1 \leqslant t' < n_s - p'$; $\Delta_s = 2p' - 2p + t' - t$; $\Delta = 0$. (e) Diagram B_2. $1 \leqslant p \leqslant n_s - 2$; $2 \leqslant t \leqslant n_s - p$; $p + 1 \leqslant p' \leqslant p + t - 1$; $n_s - p' + 1 \leqslant t' \leqslant n - p'$; $\Delta_s = n_s + p' - 2p - t$; $\Delta = p' + t' - n_s$. (f) Diagram B_3. $1 \leqslant p \leqslant n_s - 2$; $2 \leqslant t \leqslant n_s - p$; $p + 1 \leqslant p' \leqslant p + t - 1$; $n - p' + 1 \leqslant t' \leqslant n - p' + p$; $\Delta_s = n_s + 2p' - 2p - t + t' - n$; $\Delta = n - n_s$. (g) Diagram B_4. $1 \leqslant p \leqslant n_s - 1$; $n_s - p' + 1 \leqslant t \leqslant n - p - 1$; $p + 1 \leqslant p' \leqslant n_s$; $p + t - p' + 1 \leqslant t' \leqslant n - p'$; $\Delta_s = p' - p$; $\Delta = p + t' - p - t$. (h) Diagram B_5. $1 \leqslant p \leqslant n_s - 1$; $n_s - p + 1 \leqslant t \leqslant n - p$; $p + 1 \leqslant p' \leqslant n_s$; $n - p' + 1 \leqslant t' \leqslant n - p' + p$; $\Delta_s = 2p' + t' - p - n$; $\Delta = n - p - t$. (i) Diagram B_6. $1 \leqslant p \leqslant n_s - 1$; $n - p + 1 \leqslant t \leqslant n - 1$; $p + 1 \leqslant p' \leqslant n_s$; $p + t - p' + 1 \leqslant t' \leqslant n - p' + p$; $\Delta_s = 2p' - 2p +$

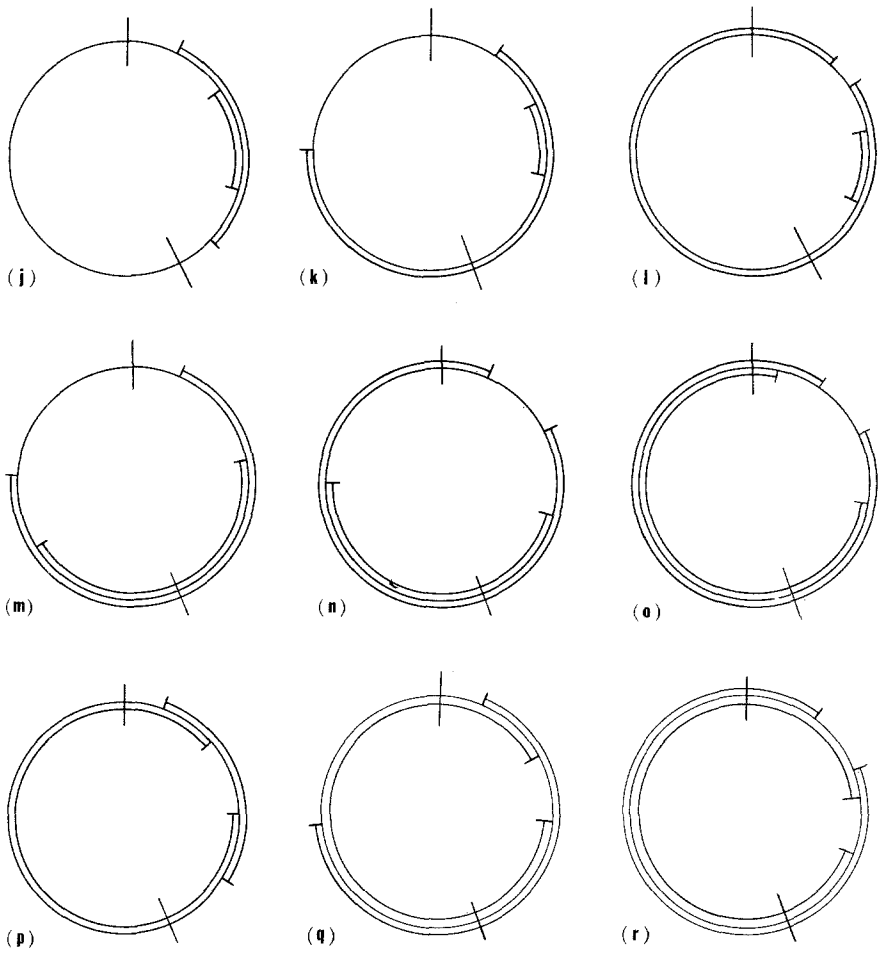

Fig. 7. Continued.

$t' - t; \Delta = 0$. (j) Diagram C_1. $1 \leqslant p \leqslant n_s - 1; 1 \leqslant t \leqslant n_s - p; p \leqslant p' \leqslant p + t - 1;$ $1 \leqslant t' \leqslant p - p' + t; \Delta_s = t - t'; \Delta = 0$. (k) Diagram C_2. $1 \leqslant p \leqslant n_s - 1; n_s - p +$ $1 \leqslant t \leqslant n - p; p \leqslant p' \leqslant n_s - 1; 1 \leqslant t' \leqslant n_s - p'; \Delta_s = n_s - t' - p; \Delta = p + t - n_s$. (l) Diagram C_3. $1 \leqslant p \leqslant n_s - 1; \; n - p + 1 \leqslant t \leqslant n; \; p \leqslant p' \leqslant n_s - 1; \; 1 \leqslant t' \leqslant$ $n_s - p'; \Delta_s = n_s - n + t - t'; \Delta = n - n_s$. (m) Diagram C_4. $1 \leqslant p \leqslant n_s; n_s - p +$ $1 \leqslant t \leqslant n - p; \; p \leqslant p' \leqslant n_s; \; n_s - p' \leqslant t' \leqslant t - p' + p; \; \Delta_s = p' - p; \Delta = p + t -$ $p' - t'$. (n) Diagram C_5. $1 \leqslant p \leqslant n_s; n - p + 1 \leqslant t \leqslant n; p \leqslant p' \leqslant n_s; n_s - p' + 1 \leqslant$ $t' \leqslant n - p'; \Delta_s = p' + t - n; \Delta = n - p' - t$. (o) Diagram C_6. $1 \leqslant p \leqslant n_s; n - p +$ $1 \leqslant t \leqslant n; \; p \leqslant p' \leqslant n_s; \; n - p' + 1 \leqslant t' \leqslant p + t - p'; \; \Delta_s = t - t'; \; \Delta = 0$. (p) Diagram D_1. $1 \leqslant p \leqslant n_s - 2; \; 2 \leqslant t \leqslant n_s - p; \; p + 1 \leqslant p' \leqslant p + t - 1; \; n - p' +$ $p + 1 \leqslant t' \leqslant n; \Delta_s = n_s - t - t' + n; \Delta = n - n_s$. (q) Diagram D_2. $1 \leqslant p \leqslant n_s - 1;$ $n_s - p + 1 \leqslant t \leqslant n - p; p + 1 \leqslant p' \leqslant n_s; n - p' + p + 1 \leqslant t' \leqslant n; \Delta_s = n - t' + p;$ $\Delta = n - p - t$. (r) Diagram D_3. $1 \leqslant p \leqslant n_s - 1; n - p + 1 \leqslant t \leqslant n; p + 1 \leqslant p' \leqslant n_s;$ $n - p' + p + 1 \leqslant t' \leqslant n; \Delta_s = 2n - t' - t; \Delta = 0$.

The integral occurring in the phase-average frequency of zeros of $f(t)$ for $k_0 = 4$ [the last expression of Eq. (21)] is

$$\int_0^\infty dx \int_0^\infty y^{-2}\, dy \int_0^T \Bigg\{ \prod_{k=1}^{4} \cos(x \cos \kappa t) \Bigg[1 - \prod_{k=1}^{4} \cos(\kappa y \sin \kappa t) \Bigg] - \sum_{\substack{k<l=1 \\ k,l \neq m,p}}^{4} \sin(x \cos \kappa t) \sin(x \cos \lambda t) \cos(x \cos \mu t) \cos(x \cos \nu t) \times \sin(\kappa y \sin \kappa t) \sin(\lambda y \sin \lambda t) \cos(\mu y \sin \mu t) \cos(\nu y \sin \nu t) - \prod_{k=1}^{4} \sin(x \cos \kappa t) \sin(\kappa y \sin \kappa t) \Bigg\} dt \tag{C.1}$$

where, for simplicity, we have ignored the restriction on the ψ_k. T is the period of $f(t)$, $\lambda = 2\pi l/n$, $\mu = 2\pi m/n$, and $\nu = 2\pi p/n$. If we compare the sizes of the contributions to the integral by the various terms in the integrand, it appears that the first term is the dominant one. The reason is that the major contribution to the integral is from small x ($< \pi/2$) when the t integral is performed over a period in t. Therefore any term containing $\sin(x \cos \kappa t)$ as opposed to $\cos(x \cos \kappa t)$ will be small because it will be of order x (rather than unity) for small values of x.

There is, however, a term in the integral for the frequency of zeros of $g(t)$,[3] which is of the form

$$\int_0^\infty dx \int_0^\infty y^{-2}\, dy \int_0^T \prod_{k=1}^{4} \cos(x \cos \kappa t) \sin(\kappa y \sin \kappa t)\, dt \tag{C.2}$$

This term appears to be as large as the leading term of Eq. (C.1) because its major contribution comes from small x. Nevertheless, it is also small because it oscillates for small y and all x. Thus the expressions for the frequency of zeros of $f(t)$ and $g(t)$ appear to have the same dominant term. Of course, a rigorous estimate of the relative size of the other terms would be desirable, but we must be content at present with the reasonable agreement with the computer "experiments" of Fig. 2.

REFERENCES

1. M. Dresden, in *Studies in Statistical Mechanics*, deBoer and Uhlenbeck, eds., North-Holland, Amsterdam (1962), Vol. 1, p. 303.
2. M. Kac, *Am. J. Math.* **65**:609 (1943).
3. N. B. Slater, *Theory of Unimodular Reactions*, Cornell University Press, Ithaca, New York (1959), p. 74.

[3] We have not written the full sum because of its sheer size. The reader can easily discern the types of terms involved.